

Accepted Manuscript

Two 4'-(4-carboxyphenyl)-3,2':6',3"-terpyridine-based luminescent Zn(II) coordination polymers for detection of 2,4,6-trinitrophenol

Jinfang Zhang, Bin Xu, Fuming Luo, Guodong Tang, Chi Zhang

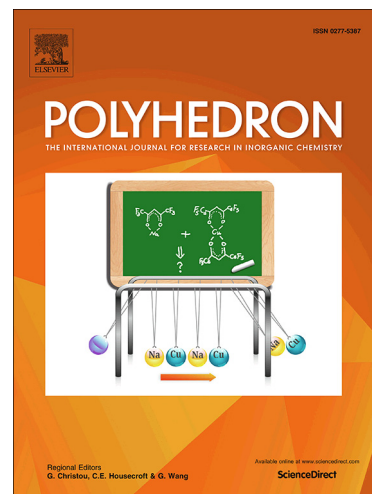
PII: S0277-5387(19)30296-7
DOI: <https://doi.org/10.1016/j.poly.2019.04.049>
Reference: POLY 13909

To appear in: *Polyhedron*

Received Date: 11 March 2019
Revised Date: 24 April 2019
Accepted Date: 25 April 2019

Please cite this article as: J. Zhang, B. Xu, F. Luo, G. Tang, C. Zhang, Two 4'-(4-carboxyphenyl)-3,2':6',3"-terpyridine-based luminescent Zn(II) coordination polymers for detection of 2,4,6-trinitrophenol, *Polyhedron* (2019), doi: <https://doi.org/10.1016/j.poly.2019.04.049>

This is a PDF file of an unedited manuscript that has been accepted for publication. As a service to our customers we are providing this early version of the manuscript. The manuscript will undergo copyediting, typesetting, and review of the resulting proof before it is published in its final form. Please note that during the production process errors may be discovered which could affect the content, and all legal disclaimers that apply to the journal pertain.



Two 4'-(4-carboxyphenyl)-3,2':6',3''-terpyridine-based luminescent Zn(II) coordination polymers for detection of 2,4,6-trinitrophenol

Jinfang Zhang^{a,*}, Bin Xu^a, Fuming Luo^a, Guodong Tang^b and Chi Zhang^{a,*}

^a International Joint Research Center for Photoresponsive Molecules and Materials, School of Chemical and Material Engineering, Jiangnan University, Wuxi 214122, PR China

^b Jiangsu Key Laboratory for Chemistry of Low-Dimensional Materials, Huaiyin Normal University, Huaian 223300, PR China

Abstract: Two new Zn(II) coordination polymers (CPs), formulated as $[Zn(3\text{-cptpy})Cl]_n$ (**1**) and $[Zn_2(3\text{-cptpy})_2(\text{DCB})(\text{H}_2\text{O})_2]_n \cdot 2n\text{H}_2\text{O}$ (**2**) (3-Hcptpy = 4'-(4-carboxyphenyl)-3,2':6',3''-terpyridine, H₂DCB = terephthalic acid), have been hydrothermally synthesized and characterized by IR spectroscopy, single-crystal and powder X-ray diffractions, and thermogravimetric analysis. **1** is constructed by Zn atoms, 3-cptpy⁻ bridges and terminal Cl ligands to form a two-dimensional (2-D) 3-connected layer structure. These layers link with each other via hydrogen bonds to form a three-dimensional (3-D) supramolecular framework. **2** displays a 1-D zigzag chain structure, which is fabricated by Zn atoms, 3-cptpy⁻ and DCB²⁻ bridges. Hydrogen bonds connect with zigzag chains to form a 3-D supramolecular architecture. **1** and **2** exhibit stronger emissions than 3-Hcptpy. Moreover, **1** shows highly sensitive and selective response to 2,4,6-trinitrophenol through luminescence quenching effect. The emission quenching mechanism of detecting TNP for **1** was explored as well.

Keywords: Zn(II) coordination polymer; crystal structure; luminescent sensor; TNP

Corresponding Author: zjf260@jiangnan.edu.cn

1. Introduction

Coordination polymers (CPs), fabricated by metal ions/clusters and bridging ligands, have rapidly constituted an interdisciplinary field [1-2] and attracted much interest due to their potential applications such as gas storage [3-5], catalysis [6-8], sensing [9-11], magnetic properties [12-14] etc. It is well-known that the self-assembly processes of CPs are greatly affected by various factors such as the nature of the ligand, coordination geometry of the metal center, reaction medium, template, metal-to-ligand ratio, pH value and counterion. 3-Hcptpy has three pyridyl and one carboxyl units, which can act as bridging groups. Therefore, it is a semi-rigid polydentate ligand, which helps to generate diverse structures for CPs. In addition, it has a large π -conjugated skeleton that helps to form a good connection between the donor and the acceptor for electron transport [15,16]. Therefore, 3-Hcptpy can act as a promising bridging ligand for building functional CPs.

With the increasing concerns about public health and environmental protection, much greater demand for the detection and removal of excessive pollutants has been urgently required [17,18]. As one of the main categories of secondary explosives, nitroaromatics (NACs) such as nitrobenzene (NB), 1,3-dinitrobenzene (1,3-DNB), 2,4-dinitrotoluene (2,4-DNB), 4-nitrotoluene (4-NT), 2,4,6-trinitrophenol (TNP) have been widely used in the fields of military, dye, agriculture, pharmaceutical industries [19,20]. Particularly, TNP has become a serious source of contamination for groundwater and soil, and has an impact on safety applications due to their explosive and highly toxic properties. Therefore, highly selective and sensitive detection of TNP is an urgent problem [21-23]. In this article, functional organic ligand 3-Hcptpy was deliberately selected to construct two distinct CPs **1** and **2**. Moreover, their luminescence and TNP sensing properties were explored.

2. Experimental Section

3-Hcptpy was prepared according to the literature method [24,25]. All chemicals and solvents were of reagent grade and were used without further purification. Powder X-ray diffraction (PXRD) data were collected on Bruker D8 ADVANCE X-

ray diffractometer with Cu-K α radiation. Steady-state fluorescence spectra were measured on a Quanta-MasterTM 40 (Photon Technology International Inc.). Thermogravimetric analyses were carried out in the temperature range 30-800 °C with a heating rate of 10 °C/min on TGA/1100SF instrument under an N₂ atmosphere. IR spectra were measured on a Nicolet 6700 FT-IR Spectrometer at room temperature.

2.1. Synthesis of [Zn(3-cptpy)Cl] **1**

A mixture of ZnCl₂ (0.0136 g, 0.1 mmol), 3-Hcptpy (0.0353 g, 0.1 mmol) and H₂O (8 mL) was stirred for 30 min in air. The reaction mixture was sealed in a Teflon-lined stainless vessel (15 mL), which was heated to 160 °C for 3 days. After cooling to room temperature at a rate of 5 °C/h, yellow crystals were obtained, washed with water and dried in air (yield: 0.0217 g, 48% based on 3-Hcptpy). IR (cm⁻¹): 3076(w), 1613(s), 1531(s), 1424(m), 1385(s), 1330(m), 1010(s), 817(m), 705(m), 659(m), 632(m).

2.2. Synthesis of [Zn₂(3-cptpy)₂(DCB)(H₂O)₂]_n·2nH₂O **2**

A mixture of Zn(NO₃)₂·6H₂O (0.060 g, 0.2 mmol), 3-Hcptpy (0.0353 g, 0.1 mmol), H₂DCB (0.016 g, 0.1 mmol) and H₂O (8 mL) was stirred for 30 min in air. The reaction mixture was sealed in a Teflon-lined stainless vessel (15 mL), which was heated to 160 °C for 3 days. After cooling to room temperature at a rate of 5 °C/h, brown crystals were obtained, washed with water and dried in air (yield: 0.0171 g, 17%, based on 3-Hcptpy). IR (cm⁻¹): 3725(m), 3627(m), 3035(m), 2341(s), 1547(s), 1481(s), 1395(m), 1280(m), 1151(m), 1095(m), 964(s), 731(s), 570(s).

2.3. Crystal structure determination

Single crystals of **1** and **2** were selected for X-ray diffraction study. Data collection was performed using a Bruker D8 VENTURE diffractometer equipped with graphite-monochromated Mo-K α radiation ($\lambda=0.71073$ Å) at 150 K. The structures were solved by direct methods and refined by a full-matrix, least-squares refinement on F² with SHELXL-2014 and SHELXT-2014 [26,27]. All non-hydrogen atoms were refined anisotropically, and hydrogen atoms were located and included at their

calculated positions. The crystal data and structural refinement parameters for **1** and **2** are summarized in Table 1. Selected bond lengths and angles are listed in Table S1 and S2. CCDC:1873508 (1); 1901836 (2).

Table 1 Crystal data and structure refinement for **1** and **2**.

	1	2
Molecular formula	C ₂₂ H ₁₄ ClN ₃ O ₂ Zn	C ₅₂ H ₃₆ N ₆ O ₁₁ Zn ₂
Formula weight	453.20	1051.61
Crystal system	monoclinic	triclinic
Space group	<i>P</i> 2 ₁ / <i>c</i>	<i>P</i> -1
<i>a</i> / Å	5.6695(11)	8.3711(2)
<i>b</i> / Å	18.935(3)	9.2910(3)
<i>c</i> / Å	16.979(3)	14.8694(4)
α / °	90	74.549(2)
β / °	95.650(7)	88.529(2)
γ / °	90	84.151(2)
<i>V</i> / Å ³	1813.9(6)	1108.88(5)
<i>Z</i>	4	1
ρ_{calc} / g cm ⁻³	1.660	1.575
<i>F</i> (000)	920	538
Reflections collected	19278	7359
GOF	1.053	1.019
<i>R</i> _{int}	0.0594	0.0215
<i>R</i> ₁ [<i>I</i> > 2σ(<i>I</i>)]	0.0300	0.0315
w <i>R</i> ₂ [<i>I</i> > 2σ(<i>I</i>)]	0.0647	0.0774

2.4. Luminescence sensing experiments

1 mg as-synthesized sample of **1** was added into 4 mL water, ethanol, methanol, trichloromethane, acetonitrile, dimethylformamide (DMF) and nitrobenzene (NB), treated by ultrasonication for 30 min, and then aged for 3 days to form stable suspensions. Detailed detections for all titrants were performed by gradually adding 5 mM DMF solution of TNP, NB, 1,3-DNB, 2,4-DNB, 4-NT, 4-NP respectively, or 5 mM H₂O solution of TNP into DMF or H₂O suspension of **1** that was placed in a 1 cm

width quartz cell with an incremental fashion. The emission spectrum of each sample was measured in the range 336-500 nm upon excitation at 326 nm. The quenching efficiency was calculated as $[I_0-I]/I_0 \times 100\%$, where I_0 and I are the luminescence emission intensities before and after addition of the analytes.

3. Results and discussion

3.1. Crystal structure of **1**

X-ray crystallography reveals that **1** belongs to the monoclinic space group $P2_1/c$ with $Z = 4$, and the asymmetric unit consists of one 3-cptpy⁻ ligand, one Zn atom and one Cl⁻ ligand (Fig. S1). Zn atom is surrounded by two O atoms from one carboxyl group, two N atoms of pyridyl from different 3-cptpy⁻ ligand and a terminal Cl⁻ to form a slightly distorted trigonal bipyramid coordination geometry (Fig. 1, S2). The bond lengths of Zn1-N2 and Zn1-N3 are 2.058(2) Å and 2.051(2) Å; the bond lengths of Zn1-O1 and Zn1-O2 are 2.0114(17) Å and 2.5409(19) Å respectively (Fig. S2). The distance of Zn1-O2 is longer than that of Zn1-O1, but it is still within the range of the reported bond distances [28]. In **1**, every 3-cptpy⁻ connects three Zn atoms with a $\mu_3-\eta^1:\eta^1:\eta^2$ mode, generating a 2-D layer structure (Fig. 1). From the topology point of view, the 2-D structure could be simplified into a 3-connected topological network with the point symbol of $(4\cdot 8^2)$, by regarding 3-cptpy⁻ and Zn centers as three connection nodes (Fig. S3). There are hydrogen bonds within layer, such as C13-H13 \cdots N1, C18-H18 \cdots Cl1, C22-H22 \cdots O2 (Fig. S4, Table S3). Neighbouring layers are linked to each other by hydrogen bonds (C17-H17 \cdots Cl1, C22-H22 \cdots O1), which results in a 3-D supramolecular framework (Fig. 2, S5). The presence of hydrogen bonds should be beneficial to the stability and luminescence property of **1**. The one-dimensional (1-D) isomer (**I**) of **1** had been reported (Fig. S6). The planar carboxylate group, benzene ring and pyridine rings of 3-Hcptpy molecule can rotate, which leads to different structures. In **1**, two N atoms of the coordinated pyridine rings from 3-cptpy⁻ bridge are in the opposite position, and Zn atom exhibits a disordered trigonal bipyramid coordination geometry (Fig. S2). In (**I**), Zn atom has the same five-coordinated mode, while two N atoms of the coordinated pyridine rings

from 3-cpty⁻ bridge are in the same position (Fig. S6), which results in a distorted square-pyramid coordination geometry for Zn atom. In **1**, the plane angle between the planar carboxylate group and the adjacent benzene ring A is 18.063(145)°; and the plane angles between the benzene ring A and the adjacent pyridine ring B is 18.956(157)° (Fig. S1). While the plane angle between adjacent pyridine rings B and C or B and D is 25.542(16)° or 24.467(179)°. In (**I**), carboxylate group, benzene ring and central pyridine ring is almost coplanar; the angle between the planes of the adjacent pyridine rings is 14.945(60)°. Therefore, 3-Hcpty ligand in **1** is more distorted than that in (**I**). Accordingly, (**I**) shows a simple 1-D chain structure, while **1** has a more complicated 2-D layer structure.

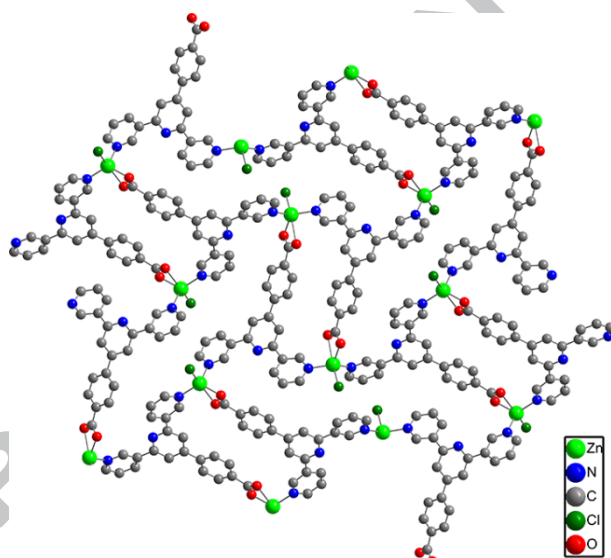


Fig. 1 A view of **1** showing the 2-D 3-connected layer structure.

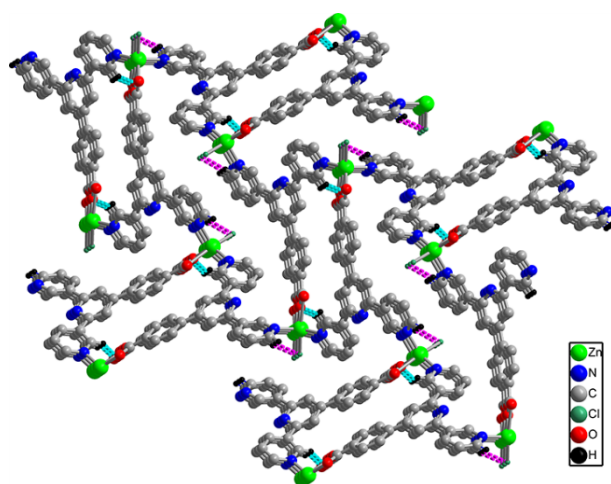


Fig. 2 A packing diagram for **1**, showing 3-D supramolecular framework based on hydrogen bonds.

3.2. Crystal structure of **2**

2 crystallizes in the triclinic space group $P-1$. The asymmetric unit consists of one Zn atom, half DCB^{2-} anion, one 3-cptpy^- ligand, one coordinated water and one lattice water (Fig. S7). Zn displays five coordinated mode, and is surrounded by one N atom from pyridyl [$\text{Zn1-N2} = 2.0424(18) \text{ \AA}$], two O atoms from 3-cptpy^- [$\text{Zn1-O1} = 2.3675(16) \text{ \AA}$, $\text{Zn1-O3} = 2.0370(15) \text{ \AA}$], one O atom from DCB^{2-} [$\text{Zn1-O4} = 1.9340(14) \text{ \AA}$] and one O atom from water [$\text{Zn1-O2} = 2.0244(15) \text{ \AA}$] to form a distorted four pyramid coordination geometry (Fig. S8). The N-Zn-O bond angles vary from $88.10(6)^\circ$ to $129.91(6)^\circ$, and O-Zn-O bond angle vary from $59.06(6)^\circ$ to $152.48(6)^\circ$. In **2**, the bridging ligands 3-cptpy^- and DCB^{2-} adopt $\mu_2\text{-}\eta_1,\eta_2$ and $\mu_2\text{-}\eta_1,\eta_1$ modes, respectively (Fig. 3). They link with Zn atoms to form 1-D zigzag chain structure, in which the $\text{Zn}\cdots\text{Zn}$ distances are 11.0929 \AA and $12.3625(3) \text{ \AA}$, respectively (Fig. 3). Hydrogen bonds [$\text{O2-H2B}\cdots\text{O3}$] connect these 1-D chains to form 2-D supramolecular network (Fig. S9), then these supramolecular networks are linked by hydrogen bonds [$\text{C17-H17}\cdots\text{O4}$] to result in a 3-D supramolecular framework (Fig. 4, Table S4).

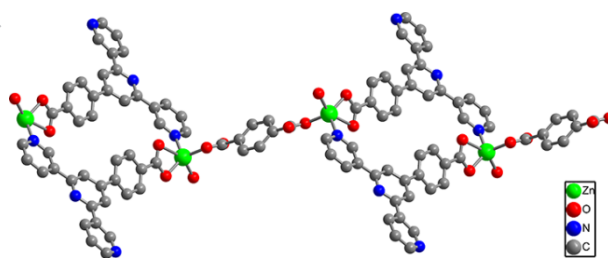


Fig. 3. A view of **2** showing the 1-D chain structure.

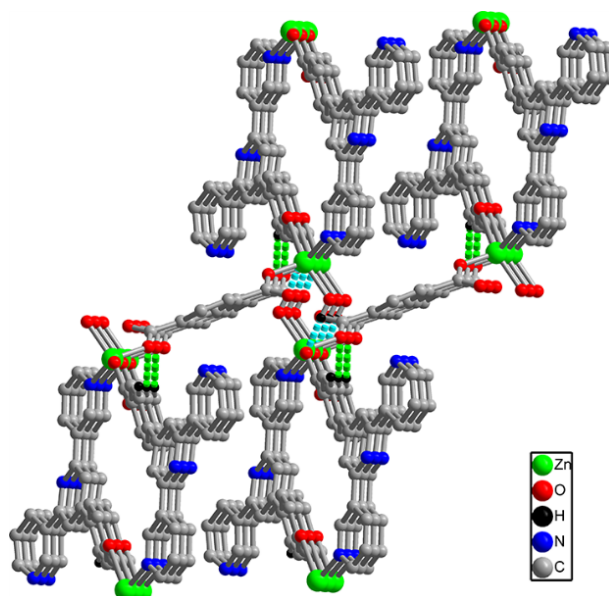


Fig. 4. A packing diagram for **2**, showing 3-D supramolecular framework based on hydrogen bonds.

3.3 Powder X-ray diffraction (PXRD) and thermogravimetric analysis (TGA)

As shown in Fig. 5 and 6, the peak positions of the experimental and simulated PXRD patterns of **1** and **2** are in good agreement, which indicates that the crystal structure of **1** and **2** is truly representative of the crystal products. To investigate the thermal stabilities of **1** and **2**, TGA were performed under a N₂ atmosphere (Fig. 7). **1** contains no solvent molecules, so there is no significant weight loss at low temperature. **1** starts to collapse at 410 °C. The rapid weight loss of **1** is caused by 3-cpty- decomposition to produce the intermediate [Zn(PhCOO)₂] [29], then the intermediate [Zn(PhCOO)₂] slowly decompose. The final residue is ZnO (found: 17.83%; calcd: 17.64%). **2** loses water molecules at 150 °C and starts to decompose at 330°C. The rapid weight loss of **2** is still caused by 3-cpty- decomposition to produce the intermediate [Zn(PhCOO)₂] [29], then the intermediate [Zn(PhCOO)₂] slowly decompose. The remaining residue corresponds to ZnO (found: 17.86%; calcd: 15.22%).

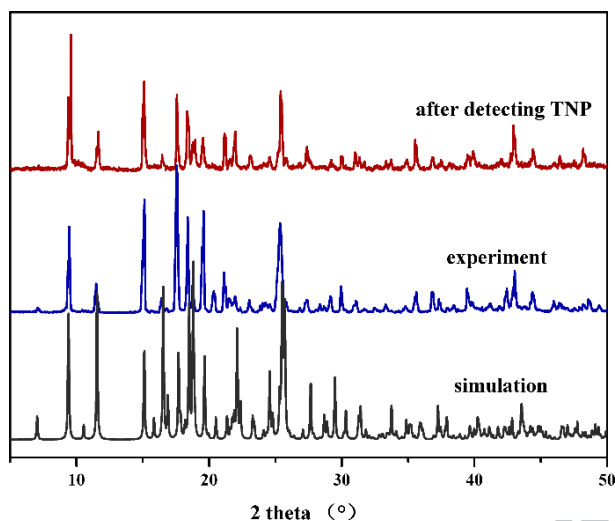


Fig. 5. Comparison of the PXRD patterns of **1**.

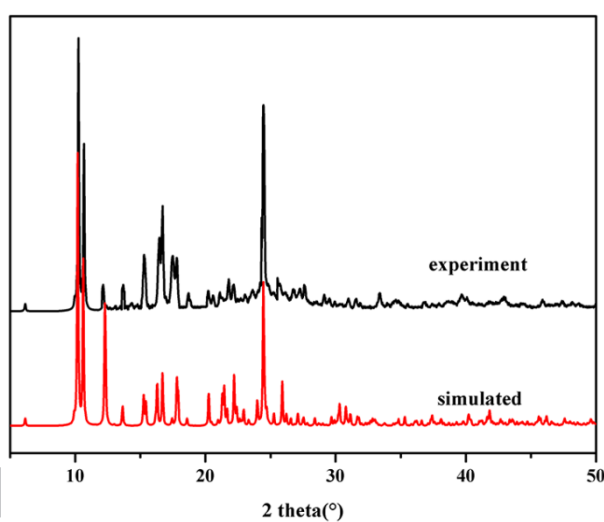


Fig. 6. Comparison of the PXRD patterns of **2**.

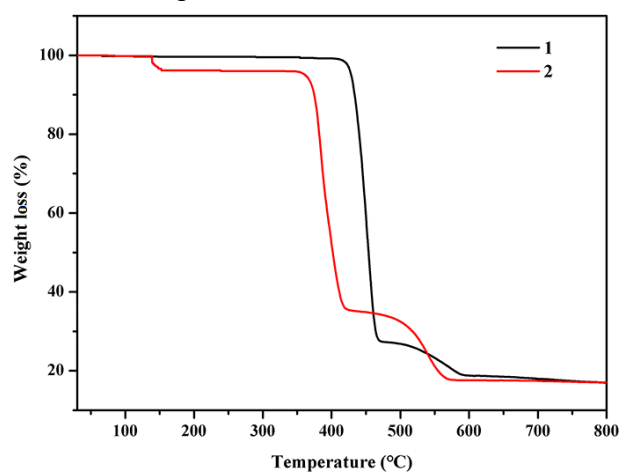


Fig. 7. Thermogravimetric analysis of **1, 2**.

3.4. Solid state luminescence

The solid-state photoluminescence properties of **1**, **2**, H₂BDC and 3-Hcptpy were

measured at room temperature. The emission bands were observed at 402 nm, 390 nm for the ligand 3-Hcpty, H₂DCB and 400 nm, 422 nm for **1**, **2** upon excitation at 290 nm, respectively (Fig. 8). In comparison with the ligand 3-Hcpty, **1**, **2** exhibits the significantly enhanced emission intensity. Because the coordination interactions between the metal ions and the organic ligands can enhance the rigidity of the ligands, decrease the loss of energy, and thereby obtain the stronger luminescence intensity of CPs [30]. The luminescence of **1** is mainly derived from 3-cpty⁻ intraligand emission [31]. Both **1** and **2** have emission peaks at 422nm, which is probably caused by ligand-to-metal charge transition (LMCT) [32]. And the emission peak of **2** at about 395 nm mainly comes from DCB²⁻ intraligand emission.

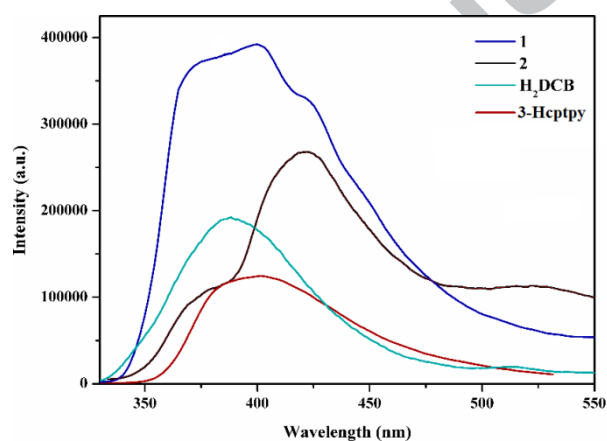


Fig. 8. The solid-state photoluminescence emission spectra of 3-Hcpty, H₂DCB, **1** and **2**, measured at room temperature.

3.5 Luminescence sensing of TNP

The effects of different solvents such as water, ethanol, methanol, trichloromethane, acetonitrile, dimethylformamide (DMF) and nitrobenzene (NB) on the luminescence intensity of **1** were investigated. 1 mg sample of **1** was dispersed in 4 mL diverse solvents with ultrasonication of 30 min to form a steady suspension. As shown in Fig. 9, **1** has the strongest luminescence intensity in the suspension of DMF. In case of NB, the luminescence of **1** is almost completely quenched. This encouraged us to study detection ability of **1** toward the other NACs, such as 1,3-DNB, 2,4-DNB, 4-NT, 4-NP and TNP. 1 mg of finely ground sample of **1** was immersed in 4 mL DMF, ultrasonicated for 24 h, aged for 2 d to prepare a stable suspension, and then gradually

added to 5 mM DMF solutions of NACs [NB, 1,3-DNB, 2,4-DNB, 4-NT, 4-NP and TNP] at room temperature. As shown in Fig. 10, the significant quenching of the luminescence intensity of **1** is observed upon addition of the selected NACs. The order of quenching efficiency is TNP > 4-NP > 4-NT > 2,4-DNB > 1,3-DNB > NB. The initial emission intensity was quenched 97.3% upon the addition of 90 μ L TNP solution. The PXRD patterns of the original sample and that obtained after TNP detection are in general agreement with each other (Fig. 5). This implies the integrity of the framework of **1** after the detection of TNP in its DMF suspension.

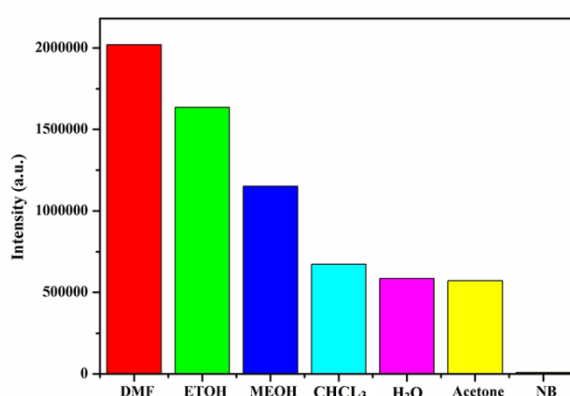


Fig. 9. Comparisons of the luminescence intensities for **1** in different organic solvents (Excitation at 326 nm).

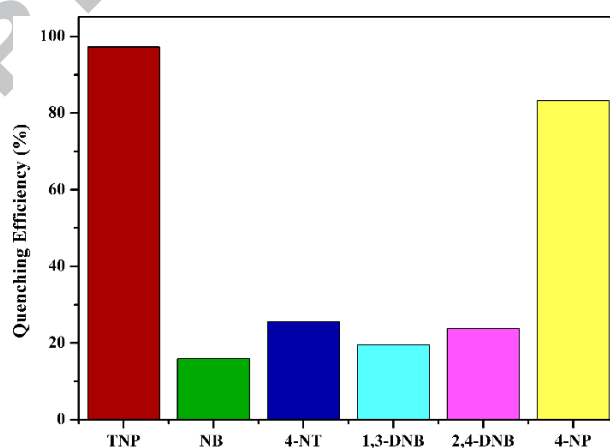


Fig. 10 Quenching efficiency of **1** upon the addition of 90 μ L of different NACs.

The luminescence quenching efficiency could be quantitatively analyzed by the Stern-Volmer equation: $(I_0/I) = K_{SV} [A] + 1$, where $[A]$ is the molar concentration of the analyte, I_0 and I are the maximum luminescent intensity of **1** before and after addition of the analyte, K_{SV} is the quenching constant. The Stern-Volmer plots for

TNP are nearly linear at low concentrations. The quenching constant (K_{SV}) for TNP is $3.86 \times 10^4 \text{ M}^{-1}$ (Fig. 11, 12), which is significantly larger than those for other NACs (4.48×10^3 , 4.8×10^3 , 6.1×10^3 , 7.1×10^3 , 2.1×10^4 for NB, 1,3-DNB, 2,4-DNB, 4-NT, and 4-NP, respectively, (Fig. S8-S17)). Furthermore, K_{SV} of **1** for TNP is higher than those of some reported CPs [33-40] (Table. 2). The detection limit of the assay calculated with $3\sigma/k$ (k : slope, σ : standard) is $2.45 \times 10^{-3} \text{ mM}$ for TNP of **1** (Fig. 13). These results reveal that **1** can act as a highly sensitive sensor for TNP.

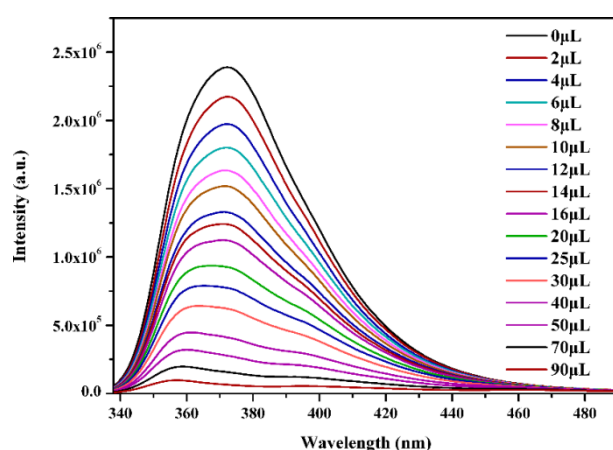


Fig. 11. Emission spectra of **1** dispersed in DMF with the addition of different volume of 5 mM DMF solution of TNP (Excitation at 326 nm).

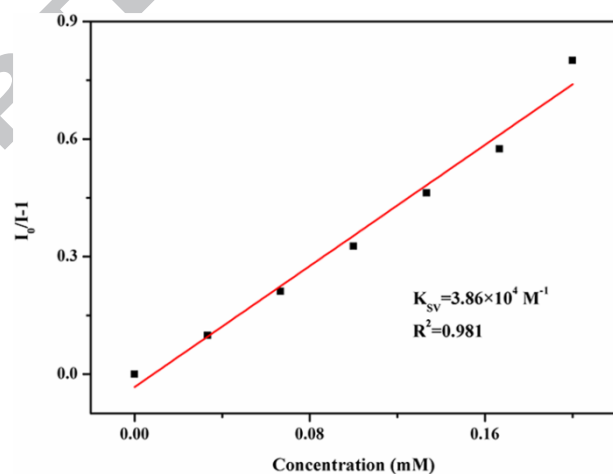


Fig. 12. Stern-Volmer plots for TNP of **1** in DMF suspensions at low concentrations (0.000-0.020 mM).

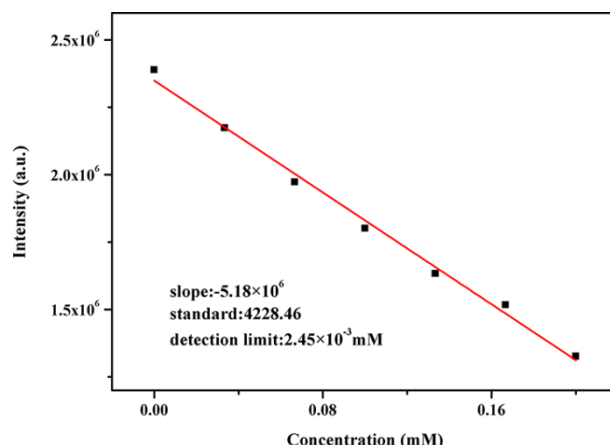


Fig. 13. The detection limits for TNP of **1** in DMF suspensions at low concentrations (0.000-0.020 mM).

Table 2. The quenching constants of the reported CPs for detecting TNP in DMF suspensions.

Molecular formula	Quenching constant (K _{sv} / M ⁻¹)	Ref.
[Zn(3-cptpy)Cl] _n	3.86 × 10 ⁴	This work
{[Cd(IPA)(L)] _n }	1.52 × 10 ⁴	[33]
{[Cd ₂ (DPBT) ₂ (BDC) ₂]·(DMA) _n }	2.83 × 10 ⁴	[34]
{[Zn ₂₄ (BDPO) ₁₂ (DMF) ₁₂]·6DMF·52H ₂ O} _n }	1.6 × 10 ⁴	[35]
[(Zn ₄ O)(DCPB) ₃]·11DMF·5H ₂ O	3.7 × 10 ⁴	[36]
[Pr ₂ (TATMA) ₂ ·4DMF·4H ₂ O]	1.6 × 10 ⁴	[37]
{[Zn ₅ (L) ₂ (DMF) ₂ (μ ₃ -H ₂ O)]·2DMF} _n }	1.84 × 10 ⁴	[38]
{(Me ₂ NH ₂)[Zn ₂ (L)(H ₂ O)]·0.5DMF}	1.42 × 10 ⁴	[39]
{[Zn ₈ (L) ₆ (μ ₃ -OH) ₄ (H ₂ O) ₆]·(DMF)·(H ₂ O) _{2.5} } _n }	2.5 × 10 ⁴	[40]

Energy transfer can significantly improve luminescence quenching efficiency and sensitivity. If the fluorophore and analyte are close to each other and the absorption band of the analyte has an effective overlap with the emission band of the fluorophore, energy transfer can occur from the fluorophore to the non-emissive analyte [41,42]. The emission spectrum of **1** has a large overlap with the absorption spectrum of TNP; this implies that the sensitive detection of TNP by **1** can be assigned to the energy transfer process (Fig. 14).

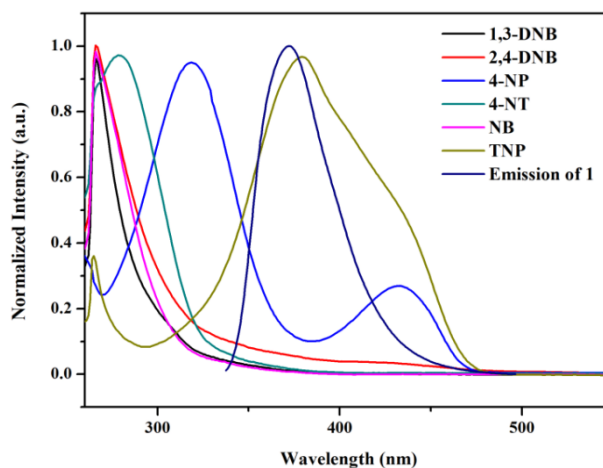


Fig. 14. Spectral overlap between the absorption spectra of NB, 1,3-DNB, 2,4-DNB, 4-NT, 4-NP, TNP and the emission spectrum of **1** in DMF media.

The selectivity of **1** toward TNP was comprehensively studied in the presence of other NACs by competition experiments. The emission spectrum for **1** dispersed in DMF is monitored upon the incremental consecutive addition of two equal portions NB solution (5 mM, 5 μ L), which results in insignificant luminescence quenching effect. Then the equal amount of aqueous TNP (5 mM, 5 μ L) is added, and its luminescence has undergone significant quenching. The trend repeats even in subsequent cycles in which NB and TNP are added. For other NACs, there is the same trend, which indicates that **1** has good selectivity for detecting TNP (Fig. 15). As shown in Fig. 14, a good spectral overlap was observed between the absorption bands of TNP and the emission of **1**, while almost no overlap was observed for NB, 1,3-DNB, 2,4-DNB and 4-NT. These results indicate that the stepwise decrease in intensity with the addition of TNP and other NACs could be caused by a different quenching mechanism [10, 43]. These results exhibit that **1** may be a promising practical TNP sensor.

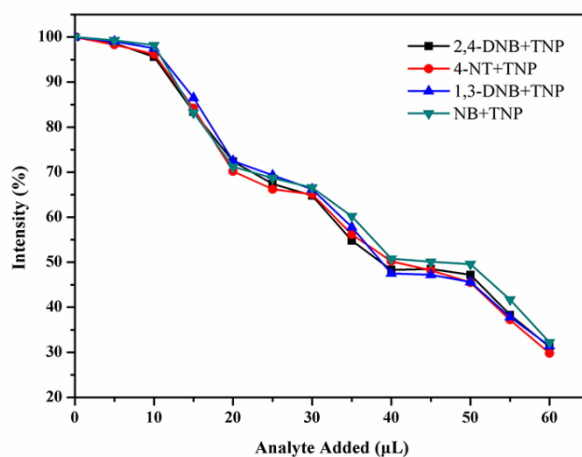


Fig. 15. Competitive luminescence quenching of **1** upon addition of other NACs followed by TNP.

Recycling experiment of **1** was also carried out. After the detection, DMF dispersion containing **1** and TNP were centrifuged. **1** was washed and dried for many times. After five cycles, the luminescence intensity of **1** was nearly constant (Fig. 16). These results indicated that **1** could be recycled after the luminescence titration experiment.

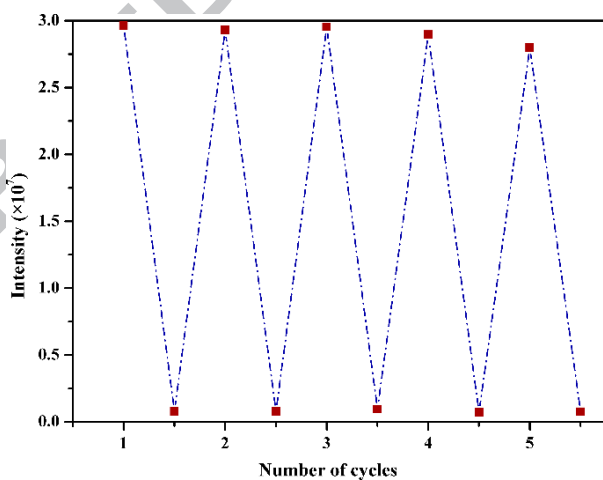


Fig. 16. Quenching and recycling experiment of **1**

NACs are released into the environment to result in the contamination of aquatic systems, thus the detection of them present in H₂O media is very important. The same luminescence quenching titration experiment as above was performed using H₂O in place of DMF. As shown in Fig. 17, the significant quenching of the emission intensity of **1** is observed upon incremental addition of an aqueous TNP solution. The

quenching efficiency can be quantitatively analyzed using the Stern-Volmer (SV) equation: $(I_0/I)=K_{sv}[A] + 1$, the quenching constant of **1** for TNP in H₂O suspension is found to be $3.8 \times 10^4 \text{ M}^{-1}$ (Fig. 18). The detection limit of the assay calculated with $3\sigma/k$ (k : slope, σ : standard) is about $8 \times 10^{-4} \text{ mM}$ for TNP of **1** (Fig. 19). These results indicate the significant potential applications of **1** for detecting TNP in aquatic systems.

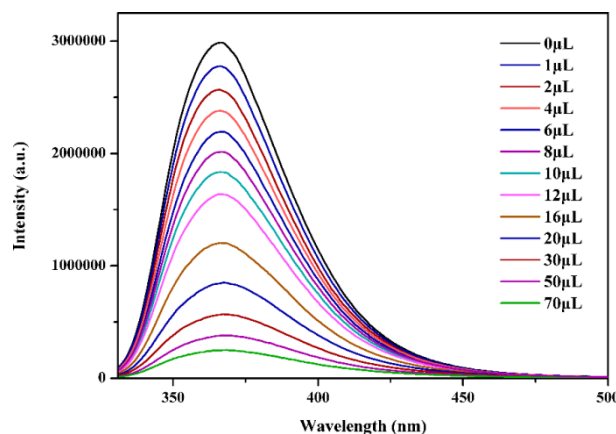


Fig. 17. Emission spectra of **1** dispersed in H₂O with the addition of different volume of 5 mM H₂O solution of TNP (Excitation at 326 nm).

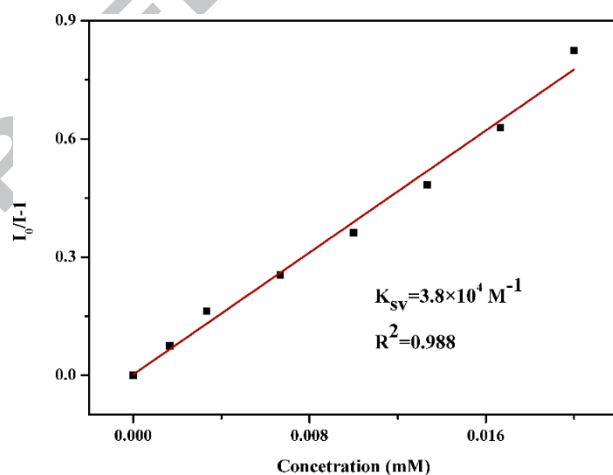


Fig. 18. Stern-Volmer plots for TNP of **1** in H₂O suspension at low concentrations (0.000-0.020 mM).

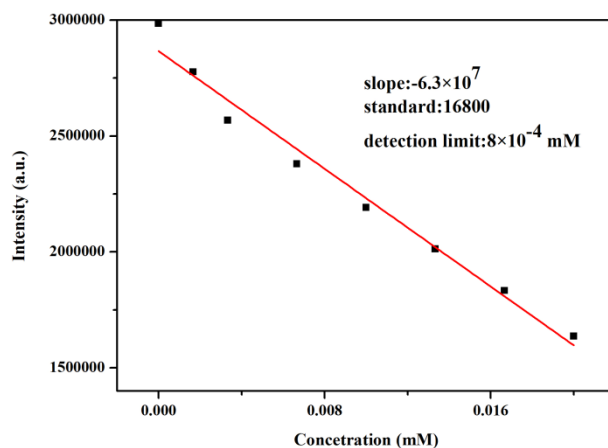


Fig. 19. The detection limits for TNP of **1** in H₂O suspension at low concentrations (0.000-0.020 mM).

4. Conclusions

In summary, two new luminescent CPs based on 3-Hcpty were successfully synthesized. **1** displays a 2-D layer architecture, and **2** shows 1-D zigzag chain structure, where 3-Hcpty bridges have distinct connected modes. **1** and **2** all form 3-D supramolecular framework through hydrogen bonds. Compared with 3-Hcpty, **1** and **2** exhibit stronger emission intensity. Moreover, **1** can highly sensitively and selectively detect TNP through luminescence quenching effect. The mechanism of **1** for the detection of TNP was elucidated. Further studies on luminescent CPs and their detection of different nitroaromatic explosives are currently in progress.

Acknowledgments

This research was financially supported by National Natural Science Foundation of China (grant No. 21671082, 51432006), Ministry of Education and the State Administration of Foreign Experts Affairs for the 111 Project (grant No. B13025), Fundamental Research Funds for the Central Universities (grant No. JUSRP51725B), Jiangsu Key Laboratory for Chemistry of Low-Dimensional Materials Foundation (grant No. JSKC17004).

References

- [1] A. Schoedel, M. Li, D. Li, M. O'Keefeand, O.M. Yaghi, Chem. Rev. 116 (2016) 12466.

- [2] K. Li, V.A. Blatov, T. Fan, T.R. Zheng, Y.Q. Zhang, B.L. Li, B. Wu, *CrystEngComm* 19 (2017) 5797.
- [3] B.J. Furlong, M.J. Katz, *J. Am. Chem. Soc.* 139 (2017) 13280.
- [4] F. Zhang, L. Hou, W. Zhang, Y. Yan, Y. Wu, R. Yang, F. Cao, Y.Y. Wang, *Dalton Trans.* 46 (2017) 15118.
- [5] C.C. Epley, M.D. Love, A.J. Morris, *Inorg. Chem.* 56 (2017) 13777.
- [6] A. Walczak, A.R. Stefankiewicz, *Inorg. Chem.* 57 (2018) 471.
- [7] B.B. Lu, J. Yang, Y.Y. Liu, J.F. Ma, *Inorg. Chem.* 56 (2017) 11710.
- [8] W.Z. Qiao, H. Xu, P. Cheng, B. Zhao, *Cryst. Growth Des.* 17 (2017) 3128.
- [9] J.F. Zhang, J.J. Wu, G.D. Tang, J.Y. Feng, F.M. Luo, B. Xu, C. Zhang, *Sens. Actuators, B.* 272 (2018) 166.
- [10] J.F. Zhang, L. Gong, J. Feng, J. Wu, C. Zhang, *New J. Chem.* 41 (2017) 8107.
- [11] X.X. Wu, H.R. Fu, M.L. Han, Z. Zhou, L.F. Ma, *Cryst. Growth Des.* 17 (2017) 6041.
- [12] Z.Y. Li, Y.Q. Cao, J.Y. Li, X.F. Zhang, B. Zhai, C. Zhang, F.L. Zhang, G.X. Cao, *Cryst. Growth Des.* 17 (2017) 6752.
- [13] H. Yao, G. Calvez, C. Daiguebonne, K. Bernot, Y. Suffren, M. Puget, *Inorg. Chem.* 56 (2017) 14632.
- [14] C. Lescop, O.G. Sibille, D.G. Mazzone, V. Ban, T. Mazet, M. François, *Inorg. Chem.* 57 (2018) 8236.
- [15] Y.L. Gai, F.L. Jiang, L. Chen, Y. Bu, M.Y. Wu, K. Zhou, J. Pan, M.C. Hong, *Dalton Trans.* 42 (2013) 9954.
- [16] N. Li, Q.E. Zhu, H.M. Hua, H.L. Guo, J. Xie, F. Wang, F.X. Dong, M.L. Yang, G.L. Xue, *Polyhedron* 49 (2013) 207.
- [17] G. Chakraborty, S.K. Mandal, *Inorg. Chem.* 56 (2017) 14556.
- [18] A.K. Chaudhari, S.S. Nagarkar, B. Joarder, S.K. Ghosh, *Cryst. Growth Des.* 13 (2013) 3716.
- [19] V. Sathish, A. Ramdass, M. Velayudham, K.L. Lu, P. Thanasekaran, S. Rajagopal, *Dalton Trans.* 46 (2017) 16738.
- [20] X.H. Guo, Y.S. Li, Q.Y. Peng, Z.M. Duan, M.X. Li, M. Shao, X. He, *Polyhedron*

133 (2017) 238.

[21] L.L. Gao, Q.N. Zhao, M.M. Li, L.M. Fan, X.Y. Niu, X.Q. Wang, T.P. Hu, *CrystEngComm* 19 (2017) 6651.

[22] M. Arici, *Cryst. Growth Des.* 17 (2017) 5499.

[23] N. Singh, U.P. Singh, R.J. Butcherb, *CrystEngComm* 19 (2017) 7009.

[24] M.W. Cooke, P. Tremblay, G.S. Hanan, *Inorg. Chim. Acta.* 361 (2008) 2259.

[25] Q.R. Wu, J.J. Wang, H.M. Hu, B.C. Wang, X.L. Wu, F. Fu, M.L. Yang, G.L. Xue, *Inorg. Chem. Commun.* 13 (2010) 715.

[26] G.M. Sheldrick, *Acta Cryst.* A71 (2015) 3.

[27] G.M. Sheldrick, *Acta Cryst.* C71 (2015) 3.

[28] S.M. Ying, J.J. Ru, W.K. Luo, *Acta Cryst.* C71 (2015) 618.

[29] L. Yang, L. Cao, X. Li, C. Qin, L. Zhao, K.Z. Shao, Z.M. Su, *Dalton Trans.* 46 (2017) 7567.

[30] F.M. Luo, G.D. Tang, J.F. Zhang, *Acta Cryst.* C74 (2018) 1133.

[31] J.F. Zhang, Y.L. Wang, W.T. Chen, L.L. Long, C. Zhang, *Z. Anorg. Allg. Chem.* 641 (2015) 1366.

[32] W.H. Huang, J. Ren, Y.H. Yang, X.M. Li, Q. Wang, N. Jiang, J.Q. Yu, F. Wang, J. Zhang, *Inorg. Chem.* 58 (2019) 1481.

[33] B. Parmar, Y. Rachuri, K.K. Bisht, R. Laiya, E. Suresh, *Inorg. Chem.* 56 (2017) 2627.

[34] K. Shen, Z.M. Ju, L. Qin, T. Wang, H.G. Zheng, *Dyes Pigm.* 136 (2017) 515.

[35] H.M. He, D.Y. Zhang, F. Guo, F. Sun, *Inorg. Chem.* 57 (2018) 7314.

[36] H.M. He, S.H. Chen, D.Y. Zhang, E.C. Yan, X.J. Zhao, *RSC Adv.* 7 (2017) 38871.

[37] H.M. He, Y. Song, F.X. Sun, Z. Bian, L.X. Gao, G.S. Zhu, *J. Mater. Chem. A* 3 (2015) 16598.

[38] J.C. Jin, X.R. Wu, Z.D. Luo, F.T. Deng, J.Q. Liu, A. Singh, A. Kumar, *CrystEngComm* 19 (2017) 4368.

[39] J. Wang, X.R. Wu, J.Q. Liu, B.H. Li, *CrystEngComm* 19 (2017) 3519.

[40] M. Gupta, D. De, S. Pal, T.K. Pal, K. Tomar, *Dalton Trans.* 46 (2017) 7619.

- [41] S.S. Nagarkar, A.V. Desai, S.K. Ghosh, *CrystEngComm* 18 (2016) 2994.
[42] L.L. Zhang, Z.X. Kang, X.L. Xin, D.F. Sun, *CrystEngComm* 18 (2016) 193.
[43] J.F. Zhang, J.J. Wu, L.P. Gong, J.Y. Feng, C. Zhang, *ChemistrySelect*. 2 (2017) 7465.

A semi-rigid polydentate ligand 3-Hcptpy was explored to construct two distinct Zn(II) coordination polymers **1** and **2**. They exhibit significantly stronger luminescence emissions than that of free 3-Hcptpy ligand. Furthermore, **1** shows highly sensitive and selective response to 2,4,6-trinitrophenol through luminescence quenching effect. The quenching mechanism of detecting TNP for **1** was explored as well.

